Deep Resources Engineering 2 (2025) 100201

Contents lists available at ScienceDirect

Deep Resources Engineering

journal homepage: www.keaipublishing.com/en/journals/deepre/

Full length article

Concept to proof long-term safety of abandoned salt mines by hydro-mechanical coupled simulations with FLAC3D and Ansys Fluent

Fabian Weber *, Heinz Konietzky

Geotechnical Institute, TU Bergakademie Freiberg, Gustav-Zeuner-Straße 1, Freiberg 09599, Germany

ARTICLE INFO

Keywords:
Salt mines
Abandoned mines
Long-term prediction
Hydro-mechanical coupling
FLAC3D
Ansys Fluent
Salt mechanics
Numerical simulation
Continuum mechanics
Computational Fluid Dynamics

ABSTRACT

Evaluation and prediction of the long-term behavior of abandoned mines have to consider complex interactions of different physical processes. The hydro-mechanical coupling plays an important role for potential short- and long-term environmental risks (e.g. surface subsidence, pollution of the biosphere, damage of the geological barrier, damage of groundwater regime). This work addresses challenges and key mechanisms in respect to long-term predictions for abandoned salt and potash mines and provides a general simulation concept. Exemplary, this concept is applied to a generic salt mine model characterized by hydro-mechanical coupling and visco-elasto as well as elasto-plastic material behavior. The concept considers time-depending rock mass and backfill material behavior. Long-lasting and large-scale fluid flow within solution-filled and backfilled cavities as well as a cavern due to creep induced convergence is simulated. A new coupling scheme between the numerical codes FLAC3D and Ansys Fluent is developed and employed for this purpose giving plausible and accurate results by efficient simulation duration. The presented workflow provides a step-by-step overview for assessing long-term safety of abandoned mines, starting with indication of main aspects determining the geomechanical and hydraulic processes followed by the exemplary model set-up, the choice of constitutive models, the simplification of the modelled mining process, the model calibration and the interpretation of the numerical results. Different model scenarios in respect to initial fluid saturation are simulated considering a partially saturated mine and a fully saturated mine, which leads to free fluid surface evolution up to the generation of excess of fluid pressure.

1. Introduction

There is an increasing interest by the society and the corresponding authorities to characterize the long-term behavior of abandoned mines and to evaluate the potential impact to the environment, especially in respect to the integrity of the geological barrier. For assessing the long-term behavior of abandoned mines usually multi-physical systems have to be investigated and the key processes have to be identified. Consideration of hydro-mechanical coupled processes is nowadays indispensable. Hydro-mechanical coupling is present in a variety of geomechnical problems e.g. hydraulic fracturing, fracture propagation and geothermal investigations [11,13,14,24,32,33] as well as slope analysis [15,28]. However, hydro-mechanical coupled assessment concepts for long-term safety of abandoned mines are rare. In the past such considerations were limited to several decades, but nowadays predictions for thousands or even millions of years are demanded. Such considerations are already widely applied for underground nuclear waste repositories (e.g. Chae, Park and Seo [2]; Claret et al. [5]; Martin, Rutqvist and Birkholzer [20]; Rutqvist and Tsang [23] or Tiedtke, Konietzky and Magri [30]), but not yet for abandoned mines. An exception is the modelling of surface movement evolution during the mine closure process (in most cases combined with flooding) in terms of long-term predictions under consideration of simplified approaches to incorporate the hydro-mechanical coupling not considering fluid flow and both-way hydo-mechanical coupling in detail, see for instance Dudek et al. [7]; Zhao and Konietzky [35] or Lüttschwager, Zhao and Konietzky [19].

In more detail investigated is the hydro-mechanical and hydro-thermo-mechanical coupled behavior of salt caverns to store gases (e.g. compressed air or hydrogen), see for instance Liu and Liu [17] or Wan et al. [31]. However, the considered timespans are limited to years or a few decades.

Abandoned mines create several potential risks, which will become even more critical if they are used for storage of toxic or environmental hazardous waste and backfill, respectively.

Potential short- and long-term environmental risks are:

* Corresponding author.
E-mail address: fabian.weber@ifgt.tu-freiberg.de (F. Weber).

https://doi.org/10.1016/j.deepre.2025.100201
Received 11 April 2025; Received in revised form 2 June 2025; Accepted 11 June 2025
Available online 9 July 2025

- Surface subsidence and uplift, which has impact on buildings, infrastructure, pipelines etc., but also on flooding, creation of wetlands or change of flow direction of rivers and streams
- Development of sinkholes, with risks to live or health, but also for properties
- Pollution of the biosphere due to damage of the geological barrier, created by mining induced movements of the overburden or generation of critical water pressures, which can trigger rock mass failure or reactivation of faults or fractures producing water pathways from the mining horizon towards the biosphere

All these potential risks are closely connected to each other. All of them are hydro-mechanical coupled and all of them are time-dependent. How can these complex processes be considered? It is impossible to consider such processes via analytical solutions or physical models based on equivalent materials. Some findings can be gained by natural analogues or the investigation of historical mines. However, such findings are mostly incomplete, very specific and cannot be directly transferred to other locations. Therefore, numerical modeling is the only choice to simulate the complex hydro-mechanical coupled long-term behavior of such complex structures. To evaluate the risks in an all-encompassing manner the complete mine including the overburden up to the surface as well as the influenced area sideward have to be included in the model.

Numerical problems arising with the hydro-mechanical coupling are: less accurate modelling of multi-physical processes or runtime issues leading to high simulation durations when using only one numerical solver or problem specific software. Numerous coupling methods of individual software codes were developed for efficient and physically precise simulation of complex hydraulic and mechanical processes interacting with each other (e.g. Rutqvist et al. [22]; Long et al. [18]; Zareidarmiyan et al., [34]; Barbi et al. [1]; Sirotti et al. [26]; Li (2021); Liu et al. [16]; Tao, Xuhai [29]; Sun et al. [27]; Cheng et al. [3], Chourdakis et al. [4]). However, none of them was developed for long-lasting and large-scale fluid flow within solution-filled and backfilled cavities experiencing creep induced convergence in order to evaluate long-term safety of abandoned salt mines.

2. Challenges

To evaluate the long-term behavior of abandoned mines comprises several aspects, which should be considered together and in their mutual interference:

2.1. Time span

Depending on type of rock mass (at mining depth, but also comprising the overburden strata), mining depth, size of mining area, geohydraulic situation and applied mining technology the time span between the date of mine closure and reaching a final stable geomechanical-geohydraulic equilibrium can be quite different. It may take centuries, but can also take much longer. One has to consider, that different processes take place with different speed and all of them have to be duplicated in a correct manner with sufficient resolution.

2.2. Hydro-mechanical coupling

The hydro-mechanical coupling plays a central role in state-of-the-art geomechanical numerical modelling. Several processes are important, like the flooding process after mine closure (increasing water level); squeezing-out of water from backfill material or fluid-filled caverns; change of saturation and creating/increase of pore or joint water pressure; change of rock properties due to wetting, saturation or pore/joint water pressure increase/decrease. Special attention has to be paid to the development of water pressure levels, which could lead to hydraulic fracturing of barrier layers.

2.3. Size of the mine

Mine workings are very complex structures with quite different layout depending on the applied mining technology. Often the excavation has taken place at several levels and the horizontal extension of the mining operation can reach several kilometers. Consequently, appropriate models should have horizontal extensions of several kilometers (often more than 10 km) and vertical extension more than maximum mining depth, which can also be up to a few kilometers. To model all the underground openings in detail for a complete mine is impossible due to the limited computer power. Therefore, simplifications (coarsening) have to be made. However, the challenge is, that these simplifications have to be done in such a way, that they reflect the underlying geomechanical and geohydraulic processes in a sufficient way.

2.4. Overburden geology

The overburden (several 100 m up to a few kilometers) is often characterized by quite different layers of rock, faults and fractures and also one or more aquifers or aquitards. This should be considered in the model; whereby special attention has to be paid to the barrier layers.

2.5. Long-term behavior of rock mass and backfill

Rock mass as well as backfill material show time-dependent behavior. Therefore, in addition to short-term parameters, processes like creep and damage evolution (sub-critical crack growth) have to be considered. These processes have also impact on the hydraulic behavior (change of permeability and porosity, built-up of pore water pressure etc.), which produce a retroactive effect on the mechanical behavior. This requires the implementation of a fully both-way hydro-mechanical coupling.

2.6. Computational time

The large model size (huge number of elements) in combination with the required both-way hydro-mechanical coupling leads to huge computational time (often weeks or months). Therefore, model optimization and/or coupling of different codes with optimal run-times for individual processes are required. There are optimized (specialized) tools for geomechanical simulations as well as for hydraulic simulations. The coupling of such codes is recommended to guarantee both, short run-times and correct duplication of the physical processes.

2.7. In-situ stress state

Besides the rockmechanical and geohydraulic parameters, the in-situ stress state has decisive influence. The primary stress state is nearly always inhomogeneous and anisotropic and difficult to measure. A lot of effort (combination of in-situ measurements and numerical stress field modelling) is necessary to obtain realistic values. However, the primary (virgin) stress field is only one part of the solution. One has also to simulate the secondary stress field. This includes to duplicate the mining process in space and time, at least in a rough manner.

3. Concept

The proposed general simulation concept is based on the following ideas (modelling sequence):

(1) Selection of appropriate numerical tools to perform the hydro-mechanical coupled simulations (coupling of codes with optimized features for solid-mechanical and fluid-mechanical modelling).

(2) Set-up a numerical model based on GIS data to replicate topography and the geological situation (layering, faults etc.) as well as the pore/joint water distribution.
(3) Implementation of the mine geometry (shafts, drifts, pillars etc.) incl. the option to insert backfill and/or support measures.
(4) Choice of appropriate constitutive models and parameters for rock mass, discontinuities, support measures and backfill material.
(5) Implementation of the in-situ stress field and appropriate boundary conditions.
(6) Duplication of the excavation process in time and space.
(7) Calibration of individual elements of the model based on in-situ measurements, for instance convergence measurements of openings, extensometer measurements in sidewalls or stress measurements in pillars.
(8) Predictive hydro-mechanical coupled modelling up to the desired point in time.

Selected key aspects of this procedure are demonstrated in a simplified manner by the following example considering a generic salt mine, which contains one salt brine cavern connected to two backfilled room-and-pillar mining fields.

4. Example

4.1. Numerical model set-up and implemented mine geometry

To demonstrate the workflow and reliability of the proposed modelling idea, a simplified generic mine located in a horizontally stratified Zechstein salinar formation is used (Fig. 1). This generic model and its stratigraphy are simplified and based on typical salt deposits in Germany [12]. For the generic model, no specific GIS data is used. However, in case of real-world applications, the usage of such data is recommended, which allows a direct transformation of the geological model into a meshed numerical model. The generic numerical model has the following dimensions: 3000 m in x-direction, 2000 m in y-direction, and represents a depth ranging from −550 m to −1080 m in the z-direction. The model comprises a total of 102,833 gridpoints (GP) and 89,865 zones. The mesh is refined progressively from the boundaries toward the mining areas.

The abandoned mine consists of two mining fields within a carnallitite layer which are developed using the room-and-pillar method, a widely used mining method in salt and potash mining. The two mining fields are connected via a drift with a deeper located, brine-filled rock salt cavern with an initial volume of 300,000 m. Fig. 1 shows a vertical cross section through the model indicating the geological layering and parts of underground excavations. Fig. 2 illustrates the two connected abstracted mining fields with the cavern in between. Vertical resolution of the mining fields and the drift is realized by two model zones only.

The mine areas are considered to be completely backfilled. The cavern is implemented as an elastic porous body with reduced elastic properties. The backfill has defined porosity, saturation, permeability and compaction behavior. The permeability of the backfill is chosen to allow relatively unrestricted drainage of brine solution. The surrounding rock mass is impermeable. Due to the viscous behavior of salt rocks, convergence occurs at the underground cavities. This convergence has two effects:

(1) Reduction of cavity volume, compaction of backfill, decreasing of porosity of the backfill material and squeezing out of fluid from the wet backfill; volume reduction of cavern connected with squeezing out of brine,
(2) Large-scale redistribution of solutions within the mine structure.

The calculation is performed for a time span of 20,000 years starting at the point in time when the mine is closed. Two scenarios are examined in detail. In the first scenario, the solutions in the mine form a free surface in the mining fields during the evaluation period (initially dry backfill). In the second scenario, a hydraulic overpressure in the mine is simulated by assuming that the backfill is initially partially saturated and the available porosity in the mining fields is insufficient to store all mobile fluids pressureless.

4.2. Selection of numerical tools

Due to the complex physical processes and boundary conditions

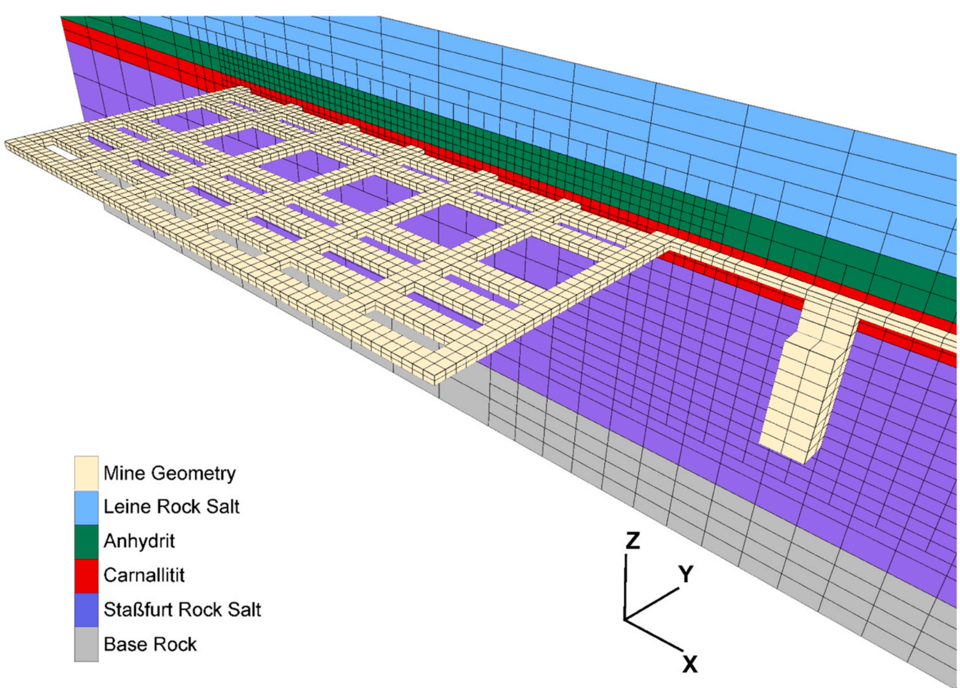

Fig. 1. Mine geometry and geological layering represented by a cross-section through the numerical model.

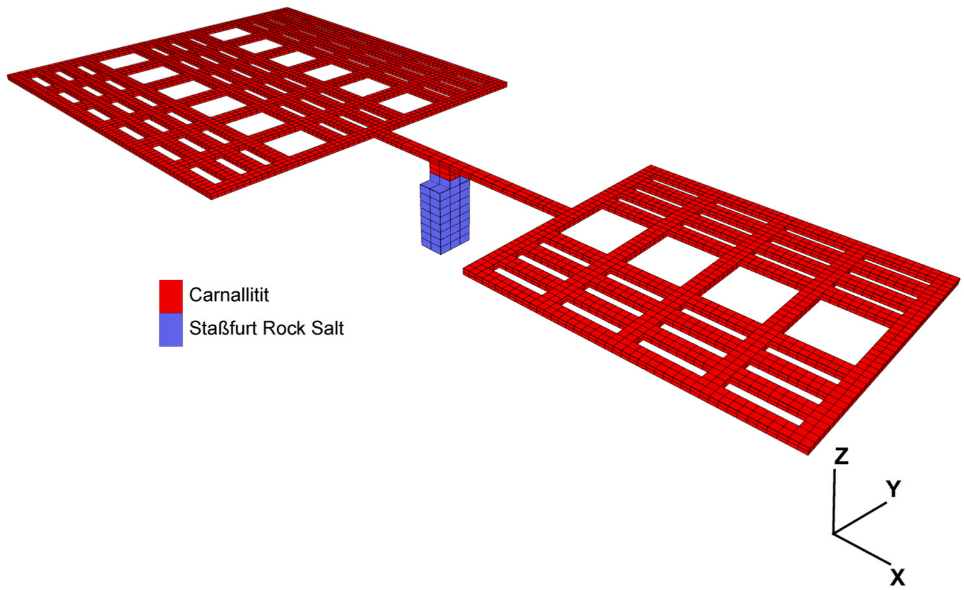

Fig. 2. Implemented mine geometry with two mining fields in carnallitite and a cavern in Staßfurt rock salt. The presented mesh is identical for FLAC3D and Ansys Fluent.

involved, empirical approaches and analytical considerations are usually unsuitable for the evaluation and numerical calculations are used instead. Special geomechanical codes (e.g., FLAC3D) can model multi-physical problems in terms of process coupling and explicit numerical schemes. This makes the numerical calculation time step and thus the duration of the numerical simulation extremely sensitive in respect to hydraulic parameters [10]. However, time-step-critical parameter constellations may arise which should be considered in the model to control fluid redistributions/flow in underground cavities, backfilled areas or man-made barriers. With evaluation periods in the order of several thousand years, this quickly leads to a dilemma between simulation duration and the accuracy of the numerical results. This can be remedied by coupling software codes which are specialized and optimized for an individual physical process. A second advantage of coupling numerical software codes is the use of their strengths to represent specific physical processes for which each individual code was developed. Therefore, software coupling ensures efficient and accurate simulations for complex multi-physics problems, like for example hydro-mechanical coupled processes.

For the numerical simulations the codes FLAC3D (mechanical part) and Ansys Fluent (hydraulic part) are used in explicitly partially two-way-coupled manner [13]. The FLAC3D-Fluent-Simulator considers laminar single-phase flow in porous media under the assumption of Darcy's law and visco-elastic and elasto-plastic behavior of the rock mass and the backfill. The simulator combines the powerful explicit geomechanical visco-elasto-plastic numerical schemes from FLAC3D with the strong implicit Computational Fluid Dynamics (CFD) from Ansys Fluent. Besides Ansys Fluent offers more complex fluid flow models as well as chemical and thermal process simulations. Therefore, the FLAC3D-Fluent-Simulator is open to simulate further coupled problems. Because the node and mesh based physical quantities are handled in both codes in a slightly different manner it was necessary to develop and to verify special transfer functions: the so-called Zone--Gridpoint-Extrapolation (ZGEx). These extrapolations transfer the hydraulic quantities saturation (s) and fluid pressure (p) from cell centers in Fluent to GP in FLAC3D. This simulator enables an accurate and time-efficient numerical simulation. Its main concept is shown in Fig. 3.

Identical meshes are used for both codes. The simulation starts with

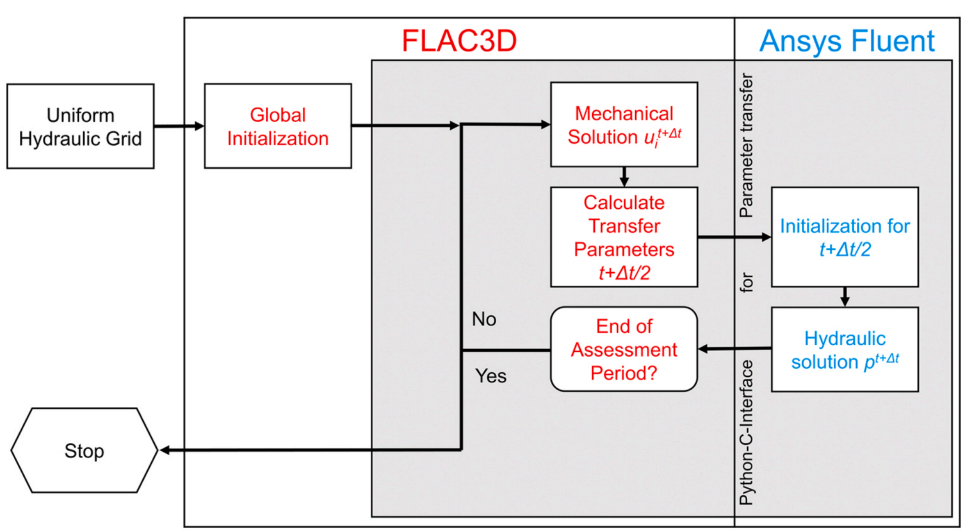

Fig. 3. Representation of the fundamental process of the FLAC3D-Fluent-Simulator for time-dependent problems.

the initialization of the FLAC3D-Fluent-Simulator. Only the hydraulically active zones receive hydraulic parameters in FLAC3D are transfered to Fluent. The model is globally initialized in FLAC3D, and the FLAC3D-Fluent-Simulator is started. FLAC3D calculates the mechanical solution $u_i^{t+\Delta t}$ (e.g. mechanical stresses and deformations) for a specified time step Δt (this can be a calculation step in FLAC3D or a defined time slice of the evaluation period e.g., 20 years). Based on the solution $u_i^{t+\Delta t}$, FLAC3D determines the necessary transfer parameters for Fluent, e.g. porosity (n), s, p and mass flow rate (m). The parameter transfer occurs for p and s in ASCII format via a Python-C interface. For n, m, and the permeability (k) Fluent-specific Profile-files are used. After calling Fluent, the transferred parameters are initialized, and the hydraulic solution $p^{t+\Delta t}$ (e.g.p and s) for the primary phase (brine/solution) is calculated. After the parameters are returned to FLAC3D, a check and possible correction of the fluid volume balance are performed to ensure volume or mass conservation during the simulation. FLAC3D then evaluates whether the end of the evaluation period has been reached to either terminate the calculation or to continue running the simulator with the next loop.

4.3. Constitutive models for rock mass and backfill

Constitutive models are implemented based on the geomechanical characteristics of each component. Table 1 summarizes the material laws applied to the individual geological units and the backfill. The overburden (Leine rock salt), the anhydrite, and the basement (a portion of the Staßfurt rock salt) are assigned linear-elastic properties. There are no cavities in these areas, therefore only elastic response is sufficient. The backfill material (crushed salt) is represented using the double-yield model, which was specifically developed for such kind of material [10]. It belongs to the class of elasto-plastic material laws and captures the stiffness increase due to compaction, necessary for simulating backfill. To model the time-dependent, visco-elastic behavior of rock salt, this study employs Norton's law [21] considering one creep mechanism (secondary creep with constant creep velocity in case of constant load) since the simulations depict very long-lasting geomechanical processes in backfilled cavities, in which the secondary creep phase is the dominant one [8].

4.4. In-situ stress field and appropriate boundary conditions

For the presented example which concentrates on the salt formations the initial stress state can be expressed as:

$$\sigma_x = \sigma_y = \lambda\sigma_z = \lambda\gamma h \tag{1}$$

Where σ_i - stress in direction i, λ – lateral earth pressure coefficient, γ – the specific weight of the overburden and h the vertical depth. Since the model depicts a series from the Zechstein salinar $\lambda = 1.0$ is considered. The use of $\lambda \neq 1.0$ for formations such as the anhydrite is possible in FLAC3D, but it has no significant impact on the hydro-mechanical simulation for the selected example and the operation of the FLAC3D-Fluent-Ssimulator.

The lower model boundary is fixed in all three spatial directions (x, y, z), while all other model boundaries, except for the top edge of the mesh, are assigned roller boundary conditions for the mechanical calculations in FLAC3D. The upper boundary is assigned a depth-related stress boundary according to Eq. (1). Fig. 4 shows a contour plot of the initial stress field (primary stress state) in a cross section of the numerical model and Fig. 5 shows a stress-depth profile indicating the correct implementation of assumptions from Eq. (1) within the numerical model. The results are from calibration simulations regarding the cavity convergence.

Table 1
Geomechanical material laws for the individual geological units implemented in the numerical model.

Material	Constitutive Law
Leine rock salt	Linear elastic
Anhydrite	Linear elastic
Carnalitite	Norton
Staßfurt rock salt	Norton
Basement	Linear elastic
Backfill	Double-Yield

4.5. Modelled excavation process and assessment period

Fig. 6 shows the principal modelling sequence. First of all, the numerical model is set-up and the proper constitutive models and parameters as well as the initial stress field and the boundary conditions are assigned. Afterwards the cavities are excavated and the cavern is filled with brine immediately, and the secondary stress state is simulated by FLAC3D. The following backfill of the abandoned mine is also performed instantaneously and the tertiary stress state is reached. Afterwards the hydro-mechanical coupled visco-elasto-plastic simulations with the FLAC3D-Fluent-Simulator start until the end of the assessment period (20,000 years). Of course, a much more detailed simulation in terms of time can be applied: for instance, a step-wise time-dependent excavation sequence or a time-dependent backfilling process. The simulations in FLAC3D can be considered as master process and the simulations in Ansys Fluent as slave process.

4.6. Model calibration and verification of ZGEx

The constitutive models and their parameters have been calibrated using various sub-models. The calibration of the creep parameters of carnallite utilizes chamber and pillar displacements as observed in a mine with similar geology and mining layout. The model displacements were compared with the results from Hampel et al. [9] in order to guarantee realistic displacement magnitudes. The primary and secondary stress state in FLAC3D, as well as the general geomechanical simulation process, are also verified (see section above about in-situ stress field). The compaction behavior of the crushed salt backfill material is calibrated based on oedometer tests and crushed salt data from Czaikowski et al. [6]. Fig. 7 shows the backfill pressure ($p_{Backfill} \triangleq$ mean stress) in relation to the volumetric strain (e) for the lab-tested material [6] and the corresponding simulation results.

To verify the ZGEx (transfer of cell variables to GP of the FLAC3D grid), a small test model was extracted from the generic mine model containing a simplified chamber within the carnalitite (Fig. 8a). Due to the viscous material behavior of the surrounding rock the chamber converges. Since the chamber is completely fluid filled from a specific point in time, FLAC3D (without using the FLAC3D-Fluent simulator) determines an excess water pressure for each zone in the chamber based on the zone-based mechanical deformations. The calculated zone water pressure is then transferred to the GP via ZGEx. Using various computational approaches, the developed ZGEx was verified with sufficient accuracy compared to FLAC3D's internal GP logic. Fig. 8 compares the pressure histories between the internal FLAC3D-GP-Logic (F3 GP-Logic) and the continuous as well as stepwise use of ZGEx for a specific zone in the chamber. Results are in good coincidence between each other.

In addition to the viscous material parameters of carnallite, the creep parameters of Staßfurt rock salt and the permeability of the cavern need to be calibrated. The FLAC3D-Fluent-Simulator for the generic mine model is used with modified model assumptions and initial conditions. No fluid flow occurs in mining panels and drift. Only the cavern and its outlet, as shown in Fig. 9a, are active in the hydraulic process of CFD. At the upper end of the outlet, a pressure boundary condition of $p = 0$ Pa is implemented in Fluent to represent an initial water level of −730 m (free surface) and to simulate the convergence-driven outflow of the brine from the cavern. The following model assumptions are considered

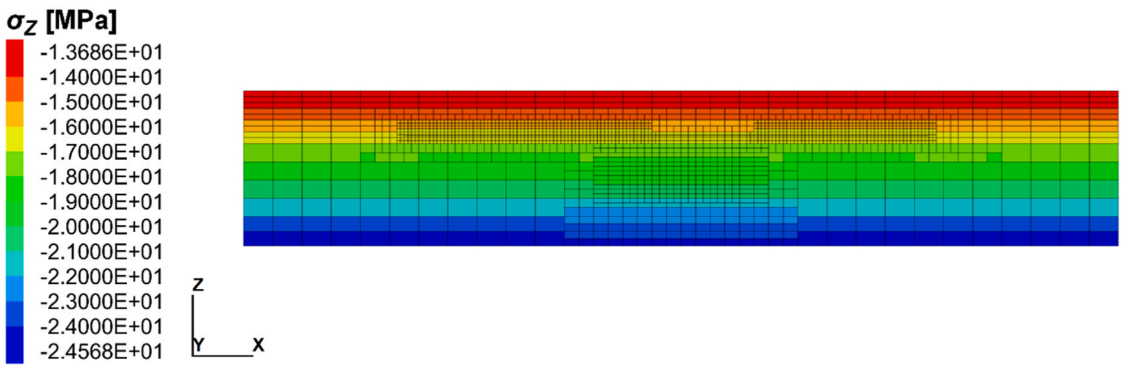

Fig. 4. Primary vertical stresses in FLAC3D along a cross-section through the model.

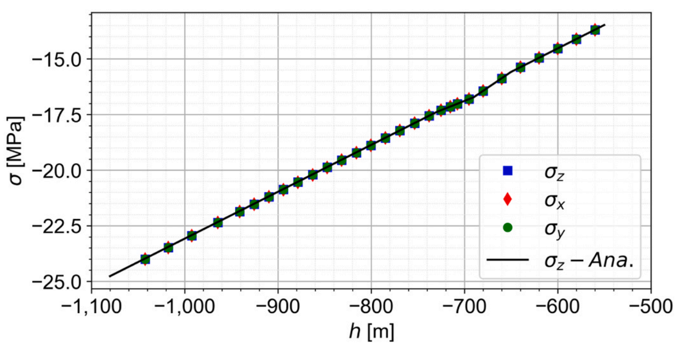

Fig. 5. Stress profiles for σ_x, σ_y, and σ_z of the primary stress state in the center of the FLAC3D model.

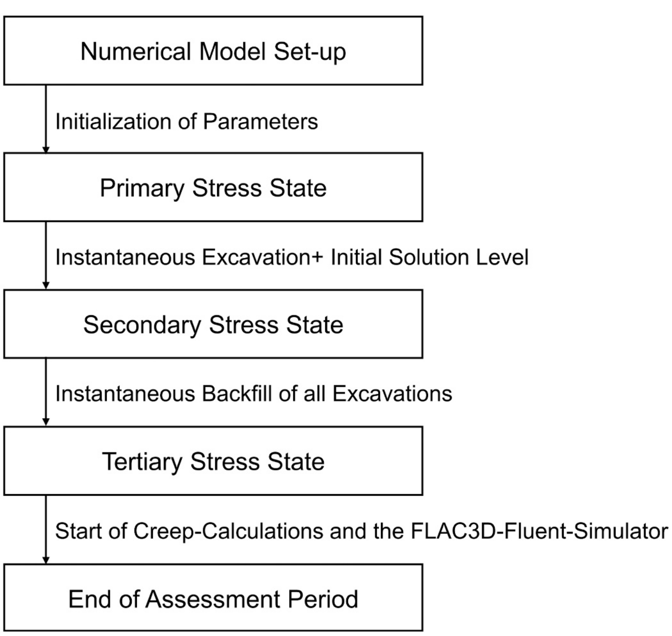

Fig. 6. Schematic simulation process for the generic mine model (master process in FLAC3D).

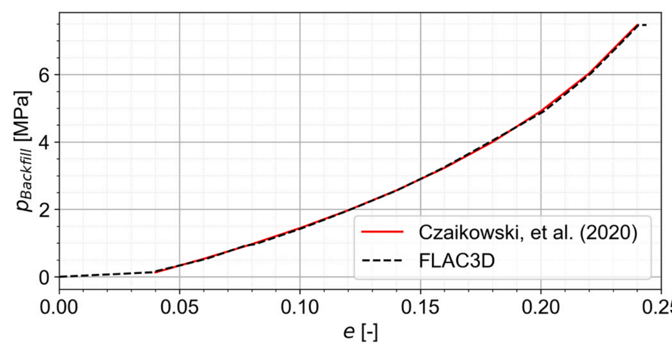

Fig. 7. Reference backfill pressure curve according to Czaikowski et al. [6] and simulated backfill pressure curve using FLAC3D.

for this simulation:

- The convergence of the cavern acts as a driving force for fluid flow.
- k is selected in such a way that no pressure build-up occurs in the cavern and the fluid pressure remains within the range of a hydrostatic pressure distribution.
- The brine freely moves inside the cavern driven by pressure boundary condition, leading to the assumption that the convergence volume of the cavern (ΔV_{Cavern}) equals the volume of brine squeezed out (ΔV_{Fluid}).
- Hydrostatic effects induced by the outflowing brine are neglected. The solution is not assumed to flow into neighboring mining areas. No adjustment of the pressure at the boundary condition is performed.

Fig. 9b illustrates the temporal development of the volume changes ΔV_{Cavern} and ΔV_{Fluid}. The cavern undergoes continuous convergence over time. Initially FLAC3D and Fluent are coupled every 20 years. After the initial time step of 20 years, the volume reduces by about 28.000 m and after 560 years the cavern is nearly fully converged (99 %). This time span is in good coincidence with a study from Shi et al. [25].

Following the calculation of mechanical time steps, the CFD simulation allows the outflow of the corresponding fluid volume through the cavern outlet. The comparison of the two volume changes reveals excellent agreement, with a maximum relative error of merely 0.05 %. Additionally, one can see the shortened time slices for coupling FLAC3D

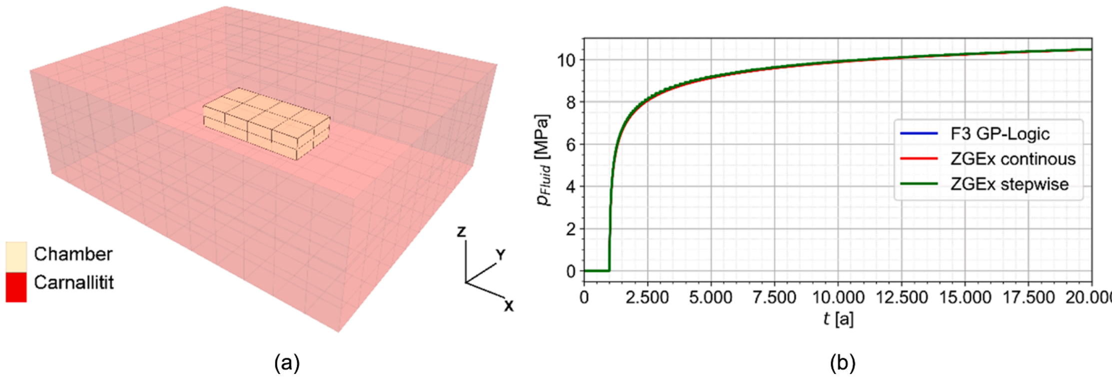

Fig. 8. Model setup of the small test model for the verification of ZGEx (a) and fluid pressure over time in a selected observation zone (b) for simulation with default FLAC3D hydraulic GP-Logic (F3-GP-Logic) as well as continuous and stepwise implementation of ZGEx.

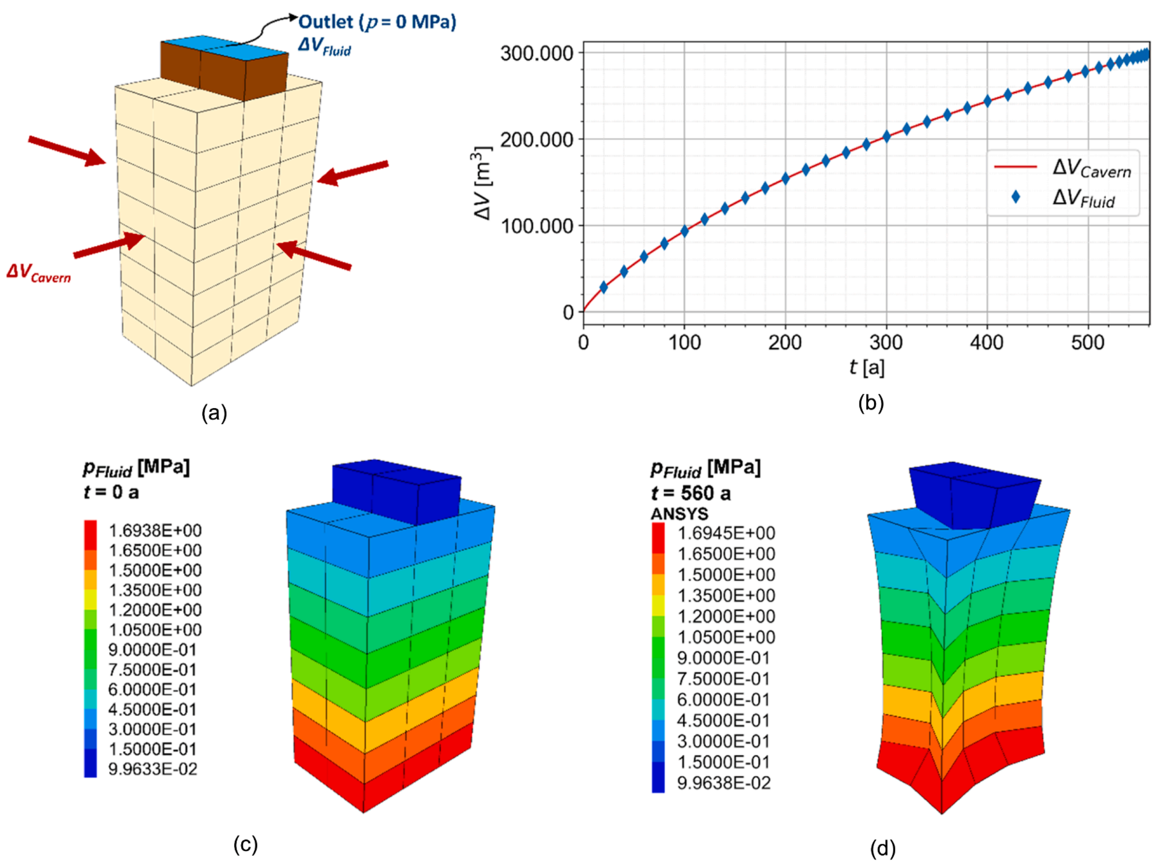

Fig. 9. Simulation results for cavern calibration with initial cavern geometry and visualization of ΔV_{Cavern} and ΔV_{Fluid} (a). Comparison of ΔV_{Cavern} and ΔV_{Fluid} show squeezed out brine corresponds to the cavern convergence (b). Fluid pressure distribution in the cavern at $t = 0$ a (c) and shortly before complete cavern convergence $t = 560$ a (d) indicates neglectable pressure increase (constant hydrostatic pressure).

and Fluent when the moment of cavern closure comes closer. This procedure is implemented in order to avoid pressure peaks within the simulation.

The initial distribution of p within the cavern at time $t = 0$ years and $t = 560$ years is illustrated in Fig. 9c and d. The contour plot clearly demonstrates the hydrostatic pressure gradient. The pressure increases linearly from 0 MPa at the pressure boundary to 1.694 MPa at the bottom of the cavern. The final distribution of p ($t = 560$ years) is similar to the initial state, with nearly no pressure build-up inside the cavern.

4.7. Simulation scenarios for the large-scale generic mine model

Three model scenarios are simulated using the generic mine model to demonstrate the application of the FLAC3D-Fluent-Simulator. They differ in terms of initial saturation and initial solution level. The first model scenario, M1, involves the simulation of a dry mine with fully backfilled mining fields and backfilled drifts as a reference case for chamber and pillar displacements. In this calculation, the cavern is free of solutions. M1 is computed solely in FLAC3D without using the

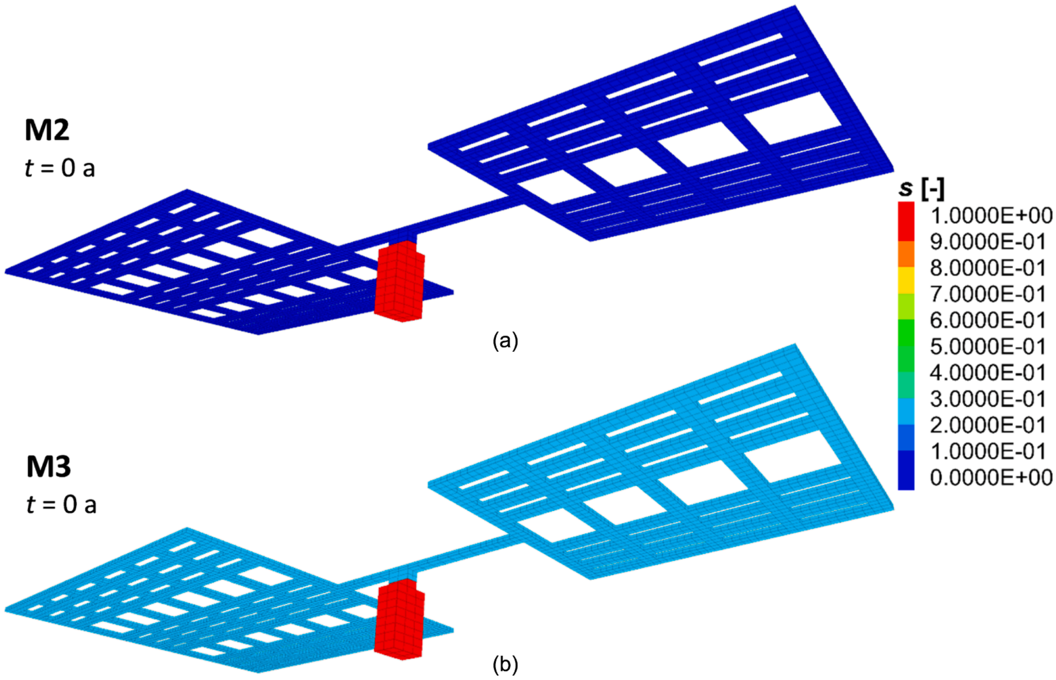

Fig. 10. Initial brine distribution in the mine in terms of saturation for model scenario M2 (a) and M3 (b).

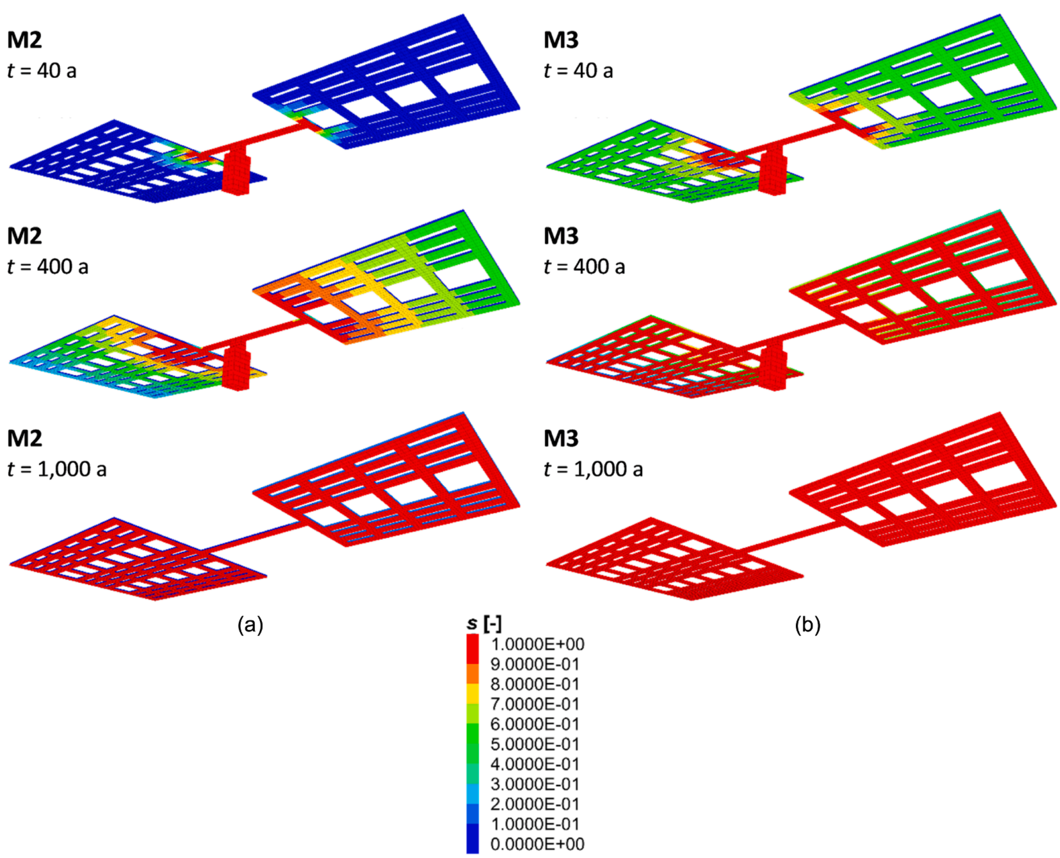

Fig. 11. Brine distribution in the mine shown in terms of saturation for $t = 40$ a, 400 a and 1000 a in scenario M2 (a) and M3 (b).

developed simulator. Model scenario M2 simulates a partially saturated mine with the initial solution level at −730 m (only cavern contains fluid), assuming dry backfill of the mining fields and dry drifts. In this case, the mine solutions can be absorbed by the mining fields almost pressure-free during the evaluation period, forming a free solution level. The final model scenario, M3, examines a partially saturated mine with an initial solution level at approximately −730 m and a wet backfill of the mining fields and drifts ($s = 0.23$). M3 simulates a fluid overpressure within the mine structure, since the porosity of the backfill is insufficient to store all mobile solutions pressure-free during the evaluation period. Fig. 10 shows the initial brine/solution saturation for M2 and M3.

4.8. Simulation results

In general convergence leads to a reduction of void space in the mining fields (backfill) and a squeezing out of brine from the cavern. The mining fields are successively filled with brine from the cavern during the assessment period. The cavern is nearly fully converged after about 600 years and is than removed from the hydraulic numerical model. The detailed evaluation of flow processes in the mine and the assessment of the distribution of solutions is carried out using contour plots of the saturation distribution and time series at selected observation points. Similar to saturation, the solution pressure is analyzed using contour plots and time series. Fig. 11 shows contour plots of the saturation for scenario M2 and M3 for selected points in time.

Due to cavern convergence, the mining fields in scenario M2 gradually fill with solutions over the course of the evaluation period. The connecting drift is filled with brine along its entire height. In the mining fields, only the junctions to the drift experience an almost complete filling up to the roof. In the remaining areas of the mining fields, a free brine level forms within the chambers and drifts, resulting in partially saturated regions ($s < 1.0$, $t = 40$ a and $t = 400$ a). After the cavern is completely converged, all brine is migrated into the mining fields forming a free surface ($t = 1000$ a). Due to geometry of the mining field the brine level is slightly higher in the smaller (right) mining field. In the larger field the solution level drops due to the cavern closure and all zones in the larger mining field are only partial filled with brine.

The fluid distribution in scenario M3 is also shown in Fig. 11b. Initially, the cavern and the drift are filled up to the solution level at approximately −730 m. The backfill has an initial saturation of 23 %. After 40 years the gravitational driven accumulation of the solutions within the backfill becomes evident. The zones near the roof are desaturated and contain no longer any solution. Due to the cavern convergence, the mining fields become filled with additional brine over the course of the evaluation period, where spatial distribution is more extensive compared to scenario M2 since there is more initial fluid volume within the model in scenario M3 ($t = 40$ a and $t = 400$ a). After the cavern is completely converged the void space in the backfill continuously reduces due to ongoing creep. After about 1000 years the void space is not anymore large enough to capture the whole solutions, all backfilled excavations are fully flooded and fluid pressure begins to increase above hydrostatic level.

Fig. 12 shows contour plots of the pressure distribution within the abandoned mine after 400 and 1000 years. For scenario M2 there is no extensive spatial pressure buildup in the mining fields during the first 400 years, as predominantly partially saturated zones are present. Minor artifacts may appear in the pressure, where pressure-free zones occur. These arise due to the definition of fully saturated zones based on threshold saturations when importing fluid pressures from Ansys Fluent into the zones since only fully saturated zone contain fluid pressure. After the cavern is converged, hydrostatic pressure conditions are present in the smaller mining field. In the larger field zones are not fully

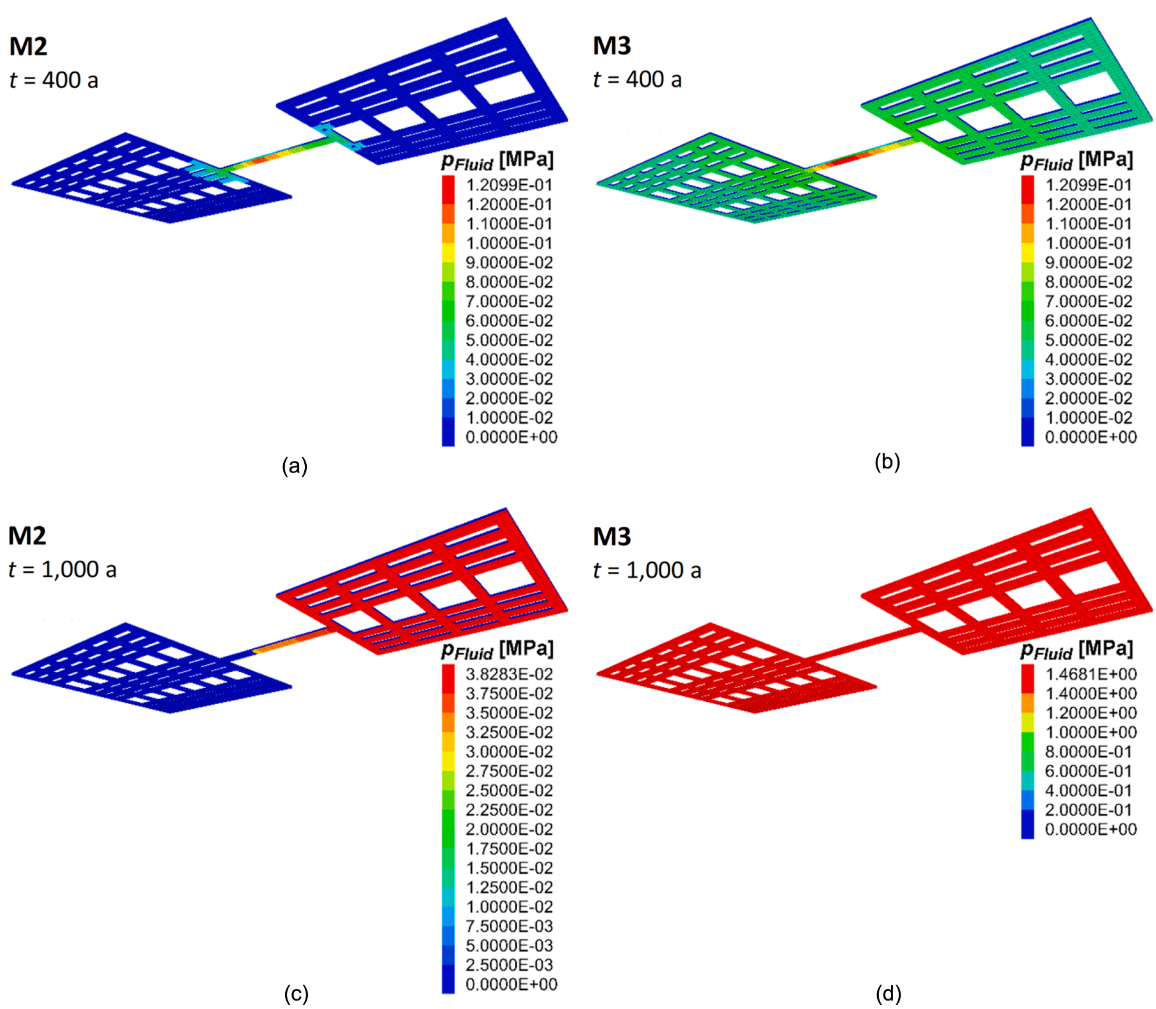

Fig. 12. Fluid pressure distribution in the mine for $t = 400$ a and 1000 a in scenario M2 and M3.

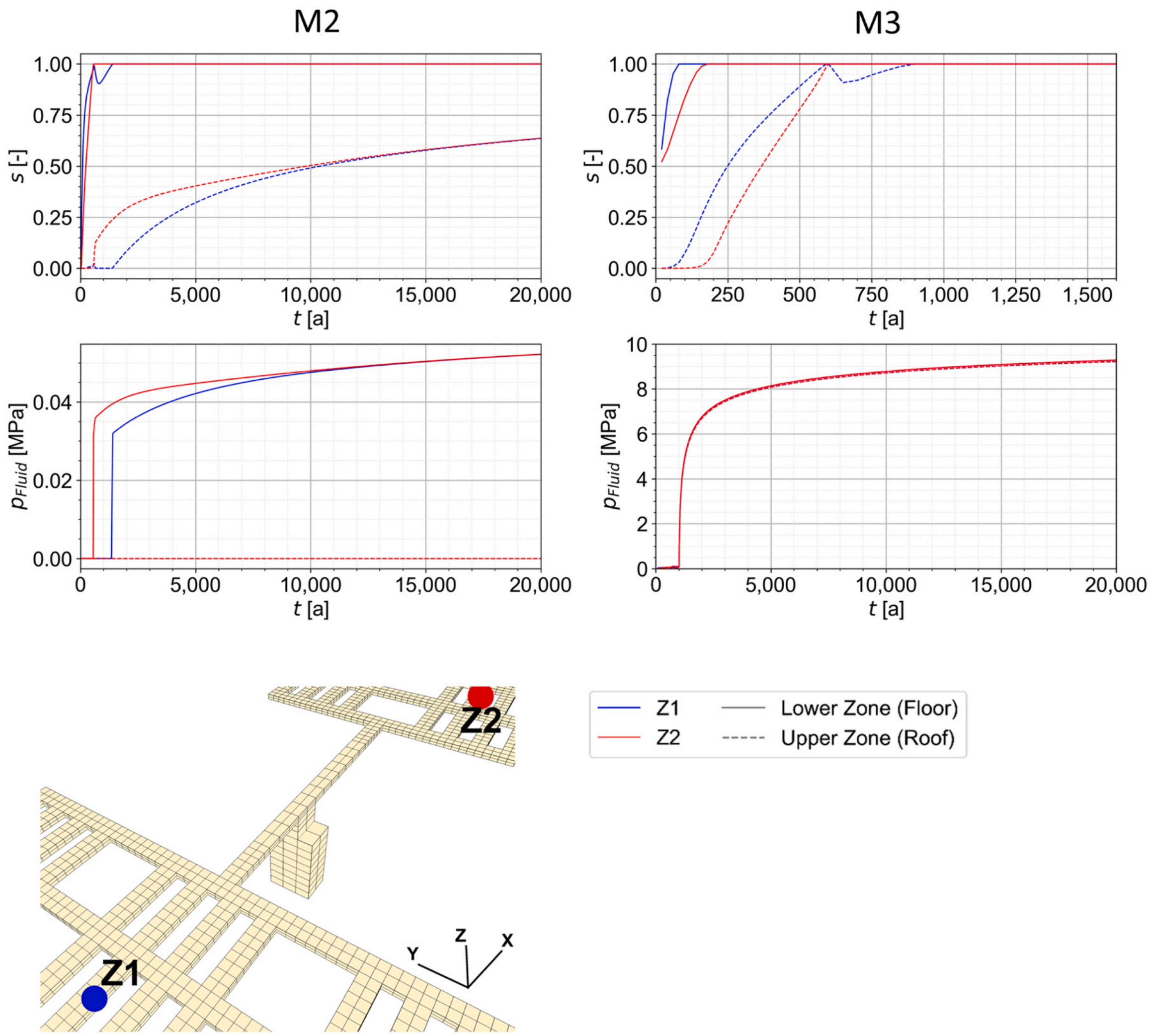

Fig. 13. Saturation and pressure histories for scenario M2 and M3 for selected zones in the mining fields.

saturated with solution or brine, therefore no pressure occurs within this area ($t = 1000$ a). Due to ongoing convergence of the excavation the solution level is raising and hydrostatic pressure condition will appear also in the larger mining field. During the assessment period solution levels in the two mining fields are equal according to hydrostatic height.

In scenario M3 the fluid pressure has already spread further into the

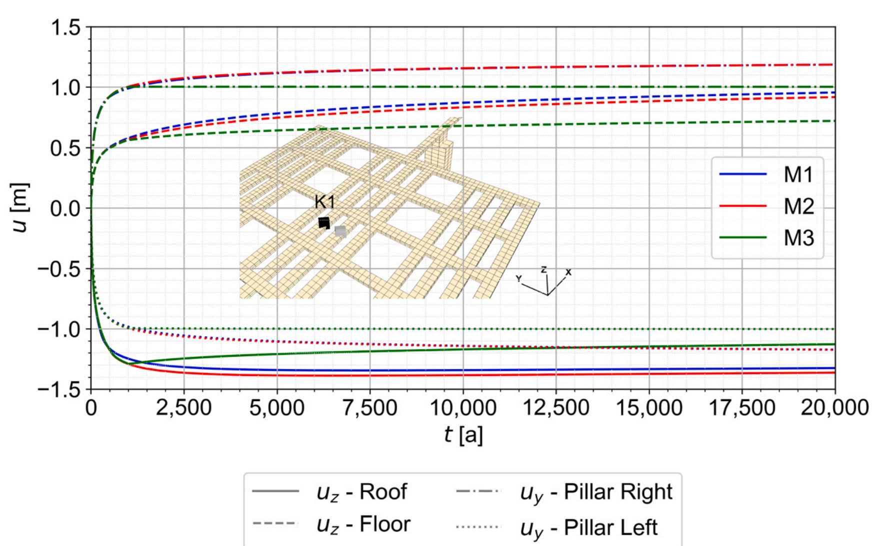

Fig. 14. Room and pillar displacements at chamber K1 for modelling scenarios M1, M2, and M3.

mining fields after 400 years compared to scenario M2. A large-scale fluid pressure distribution develops in the mining fields due to the higher solution level initiated from larger initial fluid volume. After convergence of the cavern, nearly hydrostatic conditions exist between 600 and 1000 years. Once the salt creep has compacted the backfill and all backfilled excavations are fully saturated with solution/brine, a hydraulic pressure build-up begins reaching values of 1.47 MPa after about 1000 years.

A time depending comparison of saturation and hydraulic pressure built-up for two selected observation points in the two mining fields is shown in Fig. 13. For scenario M2: in the smaller mining field (Z2) the zones near the floor (solid lines) become fully saturated more quickly than in the larger mining field (Z1). Additionally, the zones near the roof at Z2 exhibit higher saturation levels in the small mining field at the time of cavern convergence (dashed lines). After this point, desaturation occurs in the larger mining field and the solution level drops at Z1. Due to cavity convergence and outflow from the smaller field, the hydrostatic solution level at Z1 continues to rise even after cavern depletion. After approximately 10,000 years, the hydraulic conditions in the mining fields have almost completely equalized, resulting in nearly identical hydraulic heads. In scenario M3: the zones at Z1 reach full saturation more quickly than in Z2. At observation point Z2, the zone near the roof remains fully saturated even after the cavern has been depleted. The drop of the solution level at Z1 due to cavern closure is visible again, however the zones near the floor remain fully filled with solutions. After about 1000 years the remaining voids of the abandoned mine are fully filled with fluid. Pressure build-up is than initiated and the fluid pressure rise abruptly between 1000 and 2500 years followed by smaller pressure gradients until reaching about 9.3 MPa after 20,000 years.

Since the FLAC3D-Fluent-Simulator is two-way coupled, volume convergence influences fluid flow and pressure build-up lead to mechanical effects. Therefore, the chamber and pillar displacements around a selected chamber K1 are shown in Fig. 14 for the three simulated scenarios. In the first 500 years, the displacements increase almost identically in all three scenarios. The partial saturation in the backfilled chambers in M2 and M3 has not yet a significant influence on the geomechanical processes compared to the dry simulation (M1). Once the chambers are sufficiently filled with solutions in scenario M2 reduced floor heave and increased roof subsidence occur due to the gravitational effect of the solutions. The displacements in M2 remain similar to M1 until the end of the evaluation period, showing a gravitational induced offset. Once overpressure develops in model M3 the pillar displacements almost stagnate in contrast to M1 and M2. Furthermore, the pressure buildup initially slows down roof subsidence and floor heave. As the process continues, uplift effects caused by buoyancy lead to a reversal of roof displacement and a slight increase in floor heave. Compared to M1, pillar displacements are reduced by approximately 15 %, and the vertical displacements at floor and roof decrease by about 25 % and 15 %, respectively.

4.9. Simulation duration enhancement

Besides the accurate simulation of physical processes, the enhancement of calculation efficiency (runtime) was the second reason to develop the FLAC3D-Fluent-Simulator. To evaluate the efficiency improvement, in addition to the calculations in the FLAC3D-Fluent-Simulator, scenario M2 was simulated in FLAC3D only. Depending on the model parametrization and model size the simulation with the FLAC3D-Fluent-Simulator is by a factor of 10–10,000 times faster than the FLAC3D-only simulation. However, this partially extreme enhancement is observed in case of very critical time-step parameter constellations with very high permeabilities, resulting in a very small explicit time step for the hydro-mechanical coupled FLAC3D-only simulations. The performance increase applies only to the presented model and cannot be generalized or transferred directly to other problems. It depends on various factors such as:

- the hydraulic parameters,
- the zone geometry,
- the size of the time slices Δt (temporal resolution of the process),
- the number of couplings between FLAC3D and Ansys Fluent,
- the convergence behavior of the CFD calculation,

to name just a few of the influencing factors. Nevertheless, the example calculation impressively demonstrates the possibilities offered by software couplings in general and the FLAC3D-Fluent- Simulator in particular.

5. Conclusion and recommendation

Key mechanisms for assessing the long-term safety of abandoned salt mines are presented and a concept for evaluation and simulation is elaborated. The workflow of the concept is successfully applied to a simplified generic salt and potash mine with the indication of the main processes creep, backfill compaction and resulting fluid redistribution inside the excavations. A coupling method of FLAC3D and Ansys Fluent for accurate and efficient numerical simulation of a complex time-depending hydro-mechanical coupled process is developed. The proposed modelling strategy with the FLAC3D-Fluent-Simulator delivers plausible results for long-term predictions based on the calibration of individual excavation elements (pillars, caverns, chambers) and lab tests. This model strategy delivers a deeper insight into the fluid migration in abandoned and backfilled mines. Brine migrates from the cavern into the mining fields or is pressed out from the backfill material due to convergence. It allows to predict the fluid pressure built-up in space and time and to evaluate the mechanical response on room and pillar displacements. The coupling of FLAC3D and Ansys Fluent with their certain specific strengths guarantees (a) a correct physical representation of the process and (b) minimized computational time.

Possible future investigations could include:

- Detailed evaluations of underground fluid flow.
- Detecting potential hazards in respect to violation of barrier layers when pressure build-up is too large and the smallest principal stress is overcome by fluid pressure.
- Optimization of underground safety measures.
- Steering of the underground fluid flow along migration paths.

In summary the presented model strategy as well as the FLAC3D-Fluent-Simulator itself offers a variety of applications and provide the basis for creating additional value for the long-term safety assessment in geoengineering.

List of symbols

γ	Specific weight of the overburden
Δt	Timestep or time slice
ΔV_{Cavern}	Convergence volume of the cavern
ΔV_{Fluid}	Fluid outflow volume from cavern
λ	Lateral earth pressure coefficient
σ_i	Stress in direction $i = x, y, z$
h	Vertical depth
k	Permeability

m	Mass flow rate
n	Porosity
p	Pressure
$p^{t+\Delta t}$	Hydraulic solution
s	Fluid saturation of void space
t	Time
u_i	Displacements in direction $i = x, y, z$
$u_i^{t+\Delta t}$	Mechanical solution of the FLAC3D-Fluent simulator
CFD	Computational Fluid Dynamics
GP	gridpoint
ZGEx	Zone-Gridpoint-Extrapolation

CRediT authorship contribution statement

Fabian Weber: Writing – original draft, Visualization, Validation, Software, Methodology, Formal analysis. **Heinz Konietzky:** Writing – review & editing, Supervision, Conceptualization.

Declaration of Competing Interest

The authors declare that they have no known competing financial interests or personal relationships that could have appeared to influence the work reported in this paper. The author Heinz Konietzky is a member of the editorial board for Deep Resources Engineering and was not involved in the editorial review or the decision to publish this article.

References

[1] G. Barbi, A. Cervone, F. Giangolini, et al., Numerical coupling between a FEM Code and the FVM Code OpenFOAM using the MED Library, Appl. Sci. 14 (9) (2024) 3744.
[2] N. Chae, S. Park, S. Seo, Coupled mixed-potential and thermal-hydraulic model for long-term corrosion of copper canister in deep geological repository, NPJ Mater. Degrad. 7 (2023) 26.
[3] Y. Cheng, T. Wang, P. Wang, et al., Hydromechanical analysis of slurry infiltration with coupled CFD–DEM method, Numer. Anal. Method Geomech. 48 (11) (2024) 3032–3053.
[4] G. Chourdakis, D. Schneider, B. Uekermann, OpenFOAM-preCICE: Coupling OpenFOAM with external solvers for multi-physics simulations, Open. J. 3 (2023) 1–25.
[5] F. Claret, A. Dauzeres, D. Jacques, et al., Modelling of the long-term evolution and performance of engineered barrier systems, EPJ Nucl. Sci. Technol. 8 (2022) 41.
[6] O. Czaikowski, KOMPASS: Compaction of crushed salt for the safe containment (Gesellschaft für Anlagen- und Reaktorsicherheit (GRS) mbH, Hrsg.) (GRS-608). Office of Scientific and Technical Information (OSTI), 2020.
[7] M. Dudek, K. Tajduś, R. Misa, et al., Predicting of land surface uplift caused by the flooding of underground coal mines – A case study, Int. J. Rock Mech. Min. Sci. 132 (2020) 104377.
[8] R.-M. Günther, K. Salzer, T. Popp, et al., Steady-state creep of rock salt: Improved approaches for lab determination and modelling, Rock Mech. Rock Eng. 48 (6) (2015) 2603–2613.
[9] B. Leuger, R.B. Rokahr, K. Staudtmeister, et al., BMBF-Verbundprojekt: Vergleich aktueller Stoffgesetze und Vorgehensweisen anhand von 3D-Modellberechnungen zum mechanischen Langzeitverhalten eines realen Untertagebauwerks im Steinsalz, Synth. (Bundesminist. F. üR. Bild. und Forsch. (BMBF) Hrsg.) (2010).
[10] ICG, Manual FLAC3D, Itasca Consulting Group Inc, Minneapolis, Minnesota, USA, 2019.
[11] K. Jiao, D.X. Han, D.B Wang, et al., Investigation of thermal-hydro-mechanical coupled fracture propagation considering rock damage, Comput. Geosci. 26 (5) (2022) 1167–1187.
[12] K.-C. Käding, Der Zechstein in der Stratigraphischen Tabelle von Deutschland 2002, Newsl. Stratigr. 41 (1-3) (2006) 123–127.
[13] A. Lavrov, Coupling in hydraulic Fracturing simulation. In Porous Rock Fracture Mechanics, Elsevier, 2017, pp. 47–62.
[14] T.J. Li, C.A. Tang, J. Rutqvist, et al., TOUGH-RFPA: Coupled thermal-hydraulic-mechanical Rock Failure Process Analysis with application to deep geothermal wells, Int. J. Rock Mech. Min. Sci. 142 (2021) 104726 (S).
[15] X. Li, Y.N. Chen, A.L. Handwerger, et al., Dynamics of creeping landslides controlled by inelastic hydro-mechanical couplings, Eng. Geol. 317 (2023).
[16] W. Liu, J. Cheng, H.Y. Yao, et al., A micromechanical thermo-hydro-mechanical coupling model for fractured rocks based on multi-scale structures variations, Int. J. Rock Mech. Min. Sci. 170 (2023) 105545.
[17] Z.Z. Liu, Y.X. Liu, Research on the stability of salt cavern hydrogen storage and natural gas storage under long-term storage conditions, Process 12 (2024) 2080.
[18] J.P. Long, B. Zhang, B.W. Yang, et al., Review of researches on coupled system and CFD codes, Nucl. Eng. Technol. 53 (9) (2021) 2775–2787.
[19] G. Lüttschwager, J. Zhao, H. Konietzky, in: H. Konietzky (Ed.), Ground movement predictions above coal mines after flooding, 49, Geomechanik-Kolloquium, Freiberg, 2020 (Hrsg.).
[20] L.B. Martin, J. Rutqvist, J. Birkholzer, Long-term modeling of the thermal-hydraulic-mechanical response of a generic salt repository for heat-generating waste, Eng. Geol. 193 (2015) 198–211.
[21] F.H. Norton, Creep of Steel at High Tempertures, McGraw-Hill Book Company, New York, 1929.
[22] J. Rutqvist, Y.S. Wu, C.F. Tsang, et al., A modeling approach for analysis of coupled multiphase fluid flow, heat transfer, and deformation in fractured porous rock, Int. J. Rock Mech. Min. Sci. 39 (4) (2002) 429–442.
[23] J. Rutqvist, C.F. Tsang, Modeling nuclear waste disposal in crystalline rocks at the Forsmark and Olkiluoto repository sites – mechanical damage to repository excavations, Tunn. Undergr. Space Technol. 152 (2024) 105924.
[24] M. Sharafisafa, Z. Aliabadian, A. Sato, et al., Coupled Thermo-hydro-mechanical Simulation of Hydraulic Fracturing in Deep Reservoirs Using Finite-Discrete Element Method, Rock Mech. Rock Eng. 56 (7) (2023) 5039–5075.
[25] X.L. Shi, Y.P. Li, C.H. Yang, et al., Influences of filling abandoned salt caverns with alkali wastes on surface subsidence, Environ. Earth Sci. 73 (11) (2015).
[26] G. Barbi, A. Cervone, F. Giangolini, et al., Development of a Coupling Methodology Between CFD Codes, 3rd - 7h Jul 2024. In: 9th European Congress on Computational Methods in Applied Sciences and Engineering. 9th European Congress on Computational Methods in Applied Sciences and Engineering, CIMNE, 2024.
[27] L. Sun, M.J. Peng, G.L. Xia, et al., Development and validation of multiscale coupled thermal-hydraulic code combining RELAP5 and fluent code, Front. Energy Res. 8 (2021) 613852 (Artikel).
[28] V. Tagarelli, F. Cotecchia, Coupled hydro-mechanical analysis of the effects of medium depth drainage trenches mitigating deep landslide activity, Eng. Geol. 297 (2022) 106510.
[29] S.J. Tao, X.H. Tang, A coupled thermo-mechanical model based on TOUGH-FEMM for simulating thermal cracking in rocks, Pap. Presente 53rd U. S. Rock Mech. /Geomech. Symp N. Y. City N. Y. (2019). June 2019.
[30] F. Tiedtke, H. Konietzky, F. Magri, A novel DFN-DEM approach to simulate long-term behavior of crystalline rock under effects of glacial climate conditions, Deep Energy Resour. 1 (2024) 100002.
[31] F. Wan, Z.M. Jiang, X. Tian, et al., A thermo-hydro-mechanical damage model for lined rock cavern for compressed air energy storage, J. Energy Storage 78 (2024) 110186.
[32] X.Q. Wang, D.T. Lu, P.C. Li, A novel hybrid model for hydraulic fracture simulation based on peridynamic theory and extended finite element method, Theor. Appl. Fract. Mech. 123 (2023) 103731.
[33] J.J. Yu, N.Y. Li, B. Hui, et al., Experimental simulation of fracture propagation and extension in hydraulic fracturing: A state-of-the-art review, Fuel 363 (2024) 131021.
[34] A. Zareidarmiyan, H. Salarirad, V. Vilarrasa, et al., Comparison of numerical codes for coupled thermo-hydro-mechanical simulations of fractured media, J. Rock Mech. Geotech. Eng. 12 (4) (2020) 850–865.
[35] J. Zhao, H. Konietzky, Numerical analysis and prediction of ground surface movement induced by coal mining and subsequent groundwater flooding, Int. J. Coal Geol. 229 (2020) 103565.

Prof. Dr. Heinz Konietzky holds the esteemed position of a tenured professor and served many years as the head of the Institute of Geotechnical Engineering at TU Bergakademie Freiberg, Germany. His accolades include receiving the ISRM Franklin Lecture Award, chairing the Education Committee of FedIGES, and being a senior consultant for the globally recognized geotechnical software company ITASCA. Additionally, he is a member of the Czech Academy of Sciences evaluation committee, appointed expert for several mining authorities in Germany and Austria, member of the expert group for the Nuclear Inspectorate Switzerland ENSI and an editorial board member for esteemed international geotechnical journals like "Rock Mechanics and Rock Engineering" and "Journal of Rock Mechanics and Geotechnical Engineering." Prof. Konietzky's international influence is underscored by more than 200 published academic papers and leadership or participation in over 40 large-scale European and international collaborative projects. Having mentored eight Humboldt scholars from around the world, his innovative breakthroughs and outstanding contributions span diverse fields, including numerical computation, rock mechanics, and geotechnical engineering as well as material sciences and process engineering.